

Neutron cross sections for carbon and oxygen from new R-matrix analyses of the $^{13,14}\text{C}$ and ^{17}O systems

G.M. Hale^a and M.W. Paris

Theoretical Division, Los Alamos National Laboratory, Los Alamos NM 87545, USA

Abstract. We report the latest results from *R*-matrix analyses of reactions in the $^{13,14}\text{C}$ and ^{17}O systems that are of interest in reactor applications and nuclear astrophysics. These were done in order to provide separate cross sections for the stable isotopes ($^{12,13}\text{C}$) of natural carbon, and to contribute improved cross sections for ^{16}O to the CIELO project. Although particular attention was paid to the data in the standards region ($<2\text{ MeV}$) for the carbon isotopes, and to the low-energy region for $n+^{16}\text{O}$, the analyses extend to several MeV neutron energy for all the systems. The fits to the data included are generally quite good, in keeping with the unitarity constraints of *R*-matrix theory. The cross sections for $^{12,13}\text{C}$ give results for natural carbon that are close to the previous evaluation by Fu et al. at energies below 1 MeV. Above that energy, the deviations become larger, especially near the narrow resonances. The thermal cross section for ^{16}O is at the upper end of the range of recommended values, in excellent agreement with a high-precision measurement by Schneider. At higher energies, the ^{17}O analysis follows in great detail high-resolution measurements of the total cross section, and agrees quite well with the $^{13}\text{C}(\alpha,n)^{16}\text{O}$ cross section measurement of Bair and Haas at roughly their original normalization scale. We will discuss the implications of these new evaluations for critical benchmarks and astrophysical applications.

1. Introduction

Reactions in the $^{13,14}\text{C}$ and ^{17}O systems are of much interest in reactor applications and nuclear astrophysics. Since there are many oxides and carbides (as well as graphite) in reactor materials, the neutron cross sections for oxygen and carbon are of great importance. In astrophysics, the $^{13}\text{C}(\alpha,n)^{16}\text{O}$ reaction is thought to be a source of neutrons in slow-neutron (*s*-process) capture. The neutron capture cross sections for $^{12,13}\text{C}$ and ^{16}O are themselves not very well known at energies above thermal.

We have performed *R*-matrix analyses of data for these light systems in order to provide separate neutron cross sections for the stable isotopes ($^{12,13}\text{C}$) of natural carbon, and to contribute improved cross sections for $n+^{16}\text{O}$ to the CIELO project. This was done using the versatile Los Alamos *R*-matrix code EDA [1], which implements standard *R*-matrix theory [2] without any approximations. In addition, it uses the Wolfenstein density matrix formalism [3] to calculate the results of any possible measurement for two-body reactions, and relativistic kinematics throughout. The result is a description of the experimental data in terms of the usual *R*-matrix parameters (reduced-width amplitudes and eigen-energies) that ensures three basic properties of hadronic scattering theory: unitarity of the *S*-matrix, reciprocity (time-reversal invariance), and causality. These properties (especially unitarity) impose powerful constraints on the fits to the experimental data. In the following sections, we will give summaries of the data included and show the quality of the fits obtained for each of the analyses, starting

with ^{17}O . Then we will conclude with a discussion of the implications of the new cross sections for various applications.

2. ^{17}O system analysis

The ^{17}O system analysis included all possible reactions between the channels $n+^{16}\text{O}$ and $\alpha+^{13}\text{C}$. This is summarized in Table 1. Particular attention was paid to the data in the low-energy region for $n+^{16}\text{O}$, shown in Fig. 1. The thermal cross section is lower than before, but still at the upper end of the range of recommended values, in excellent agreement with a high-precision measurement by Schneider [4]. At higher energies, as shown in Fig. 2, the ^{17}O analysis follows in great detail the total cross section measurements of Ohkubo [5], Johnson [6], Fowler [7], and Cierjacks [8] with reasonable re-normalizations (-2% to $+4\%$). It also agrees quite well with the $^{13}\text{C}(\alpha,n)^{16}\text{O}$ cross section measurement of Bair and Haas [9] at roughly their original normalization scale (0.94), a consequence of the unitarity imposed by an *R*-matrix description. The resulting $^{16}\text{O}(n,\alpha)^{13}\text{C}$ cross sections are shown in Fig. 3. They agree with the measurements and evaluation done at IRMM by Giorganis [10], which are 30 – 40% higher than the ENDF/B VII.1 cross sections.

3. $^{13,14}\text{C}$ system analyses

The ^{13}C system analysis included reactions among the channels $n+^{12}\text{C}$, $n+^{12}\text{C}^*$, and $\gamma+^{13}\text{C}$. A summary of the channel configuration and data for the reactions included is given in Table 2. Although particular attention was paid to the data in the standards region ($E_n < 2\text{ MeV}$) for the

^a e-mail: ghale@lanl.gov

Table 1. Channel configuration (top) and data summary (bottom) for the ^{17}O analysis. Chi-squared per degree of freedom for the analysis is 1.68.

channel	a_c (fm)	l_{max}
$n+^{16}\text{O}$	4.4	4
$\alpha+^{13}\text{C}$	5.4	3

reaction	energy range (MeV)	# data points	observables
$^{16}\text{O}(n, n)^{16}\text{O}$	$E_n = 0-7$	2540	$\sigma_T, \sigma(\theta), P_n(\theta)$
$^{16}\text{O}(n, \alpha)^{13}\text{C}$	$E_n = 2.35-5$	672	$\sigma_{int}, \sigma(\theta), P_n(\theta)$
$^{13}\text{C}(\alpha, n)^{16}\text{O}$	$E_\alpha = 0-5.4$	870	σ_{int}
$^{13}\text{C}(\alpha, \alpha)^{13}\text{C}$	$E_\alpha = 2-5.7$	1168	$\sigma(\theta)$
total:		5250	8

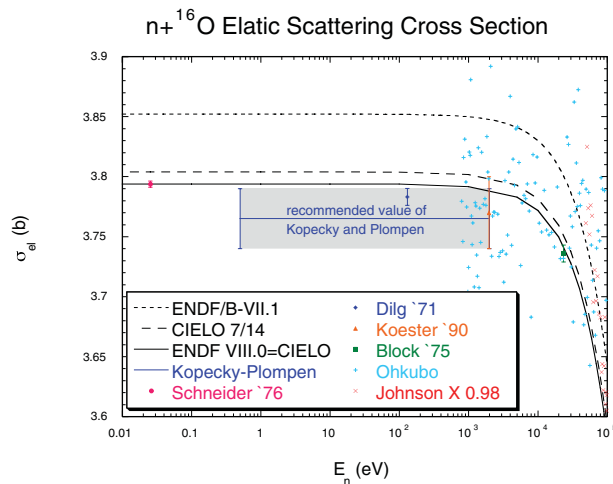


Figure 1. Low-energy cross sections for $n+^{16}\text{O}$ elastic scattering. The dotted curve is ENDF/B VII.1, the dashed curve is an earlier CIELO version, and the solid curve is ENDF/B VIII.0.

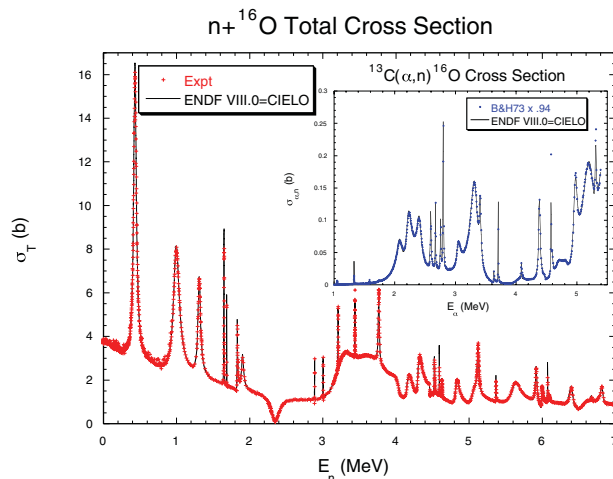


Figure 2. $n+^{16}\text{O}$ total cross section compared to experimental data [5–8]. The insert shows the fit to the $^{13}\text{C}(\alpha, n)$ measurement of Bair and Haas [9], renormalized by 0.94.

carbon isotopes, the analyses extend to several MeV for both the $^{13,14}\text{C}$ systems. The types of data used are mostly differential and integrated (total) cross sections, but some analyzing-power measurements are also included. The fits to the data are generally quite good, as can be seen in Figs. 4 and 5. Some changes were also made in the $n+^{12}\text{C}$

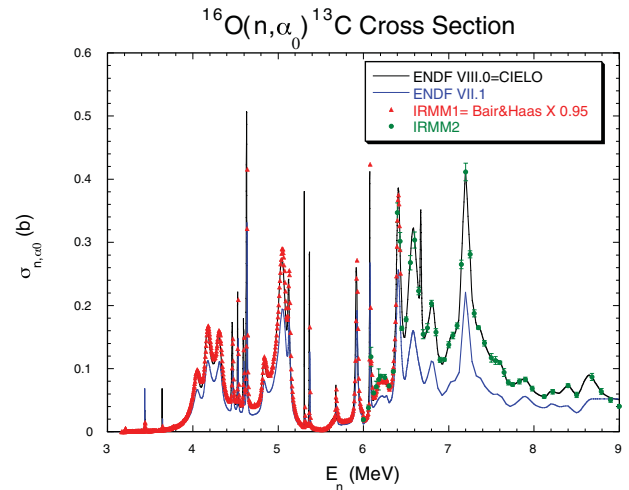


Figure 3. Cross sections for the $^{16}\text{O}(n, \alpha)^{13}\text{C}$ reaction. The blue curve is ENDF/B VII.1, the black curve is ENDF/B VIII.0, and the data points are from the IRMM measurements [10].

Table 2. Channel configuration (top) and data summary (bottom) for the ^{13}C analysis. Chi-squared per degree of freedom for the analysis is 1.54.

channel	a_c (fm)	l_{max}
$n+^{12}\text{C}(0^+)$	4.6	4
$n+^{12}\text{C}^*(2^+)$	5.0	1
$\gamma+^{13}\text{C}$	50.	1

reaction	energy range (MeV)	# data points	observables
$^{12}\text{C}(n, n)^{12}\text{C}$	$E_n = 0-6.45$	6940	$\sigma_T, \sigma(\theta), A_n(\theta)$
$^{12}\text{C}(n, n')^{12}\text{C}^*$	$E_n = 5.3-6.45$	443	$\sigma_{int}, \sigma(\theta)$
$^{12}\text{C}(n, \gamma)^{13}\text{C}$	$E_n = 0-0.2$	7	σ_{int}
total:		7390	5

capture cross section, as can be seen in Fig. 6. The flat region between 0.2 and 7 MeV in ENDF/B VII.1 has been replaced with a more physically reasonable behavior when joined to the higher-energy data above 10 MeV.

The $n+^{13}\text{C}$ (^{14}C system) analysis has been done in two versions. The first was a single-channel analysis that went only up to 5 MeV. That analysis included total cross section data and differential cross sections for elastic scattering. A preliminary ENDF/B evaluation for ^{13}C based on this analysis, which also included the capture cross section, was submitted in August of 2015. The second analysis was completed recently for inclusion in ENDF/B VIII.0. It is a six-channel analysis that goes up to 20 MeV, but includes experimental data only for the total cross section. The results from that analysis are shown in Fig. 7. The total cross section from that analysis is similar to the one obtained earlier at energies below 5 MeV.

4. Natural carbon

These cross sections for $n+^{12,13}\text{C}$ combine to give results for natural carbon that are very close to the previous evaluation (ENDF/B VII.1) by Fu *et al.* at energies below 1 MeV. Between 1 and 2 MeV, the deviations become larger, approaching 2% just below the first resonance, and are even larger at higher energies, especially near the narrow resonances.

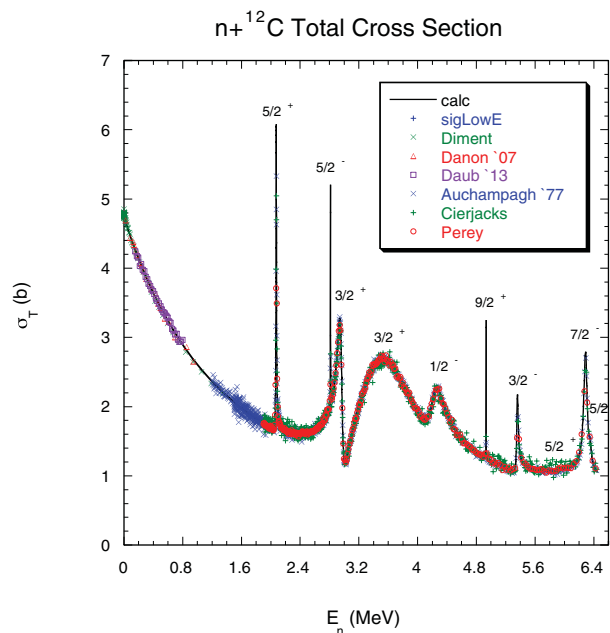


Figure 4. Total cross section for $n+^{12}\text{C}$ compared to experimental data. The J^π values of the resonances are indicated above the peaks.

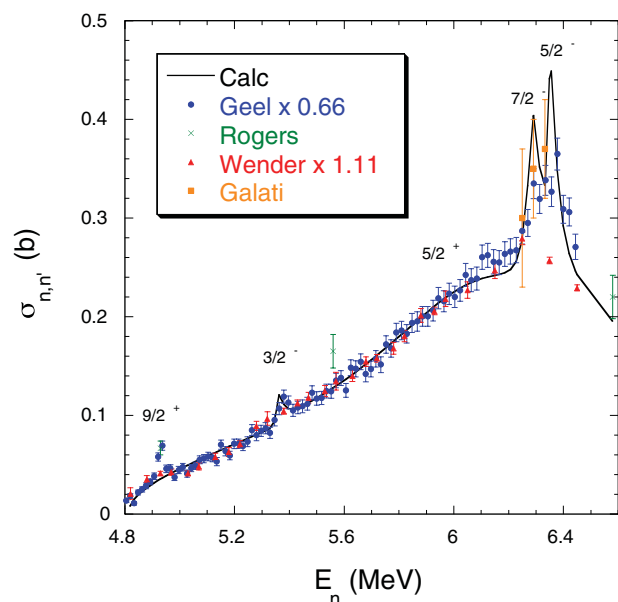


Figure 5. Cross section for $n+^{12}\text{C}$ inelastic scattering to the first level compared to experimental data. The J^π values of the resonances are indicated above the peaks.

Earlier this year, Andrej Trkov (IAEA) merged the 2015 ENDF/B file for ^{13}C with the TENDL file at energies above 5 MeV to produce an evaluation that extends to 150 MeV. Using those cross sections with the new ones for ^{12}C , he made a plot of the $n+^{\text{nat}}\text{C}$ elastic scattering cross section that is shown in Fig. 8. The error bars on the measured data are large, but they tend to support the trend of the new ^{12}C cross section to higher values in the region below 2 MeV. On the other hand, a recent measurement of the total cross section by Danon (RPI) that was not included in the ^{13}C analysis appears to support the lower cross sections in this energy region.

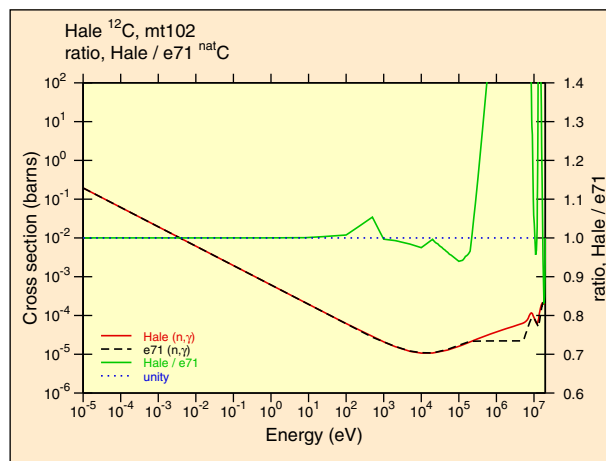


Figure 6. Cross sections for $n+^{12}\text{C}$ capture. The dotted black curve is ENDF/B-VII.1 and the new cross section is the red curve. The green curve gives the ratio to ENDF/B-VII.1 (figure courtesy of Skip Kahler).

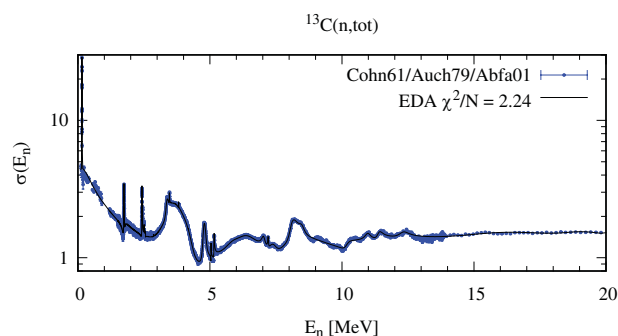


Figure 7. Total cross section for $n+^{13}\text{C}$ compared to experimental data at energies up to 20 MeV.

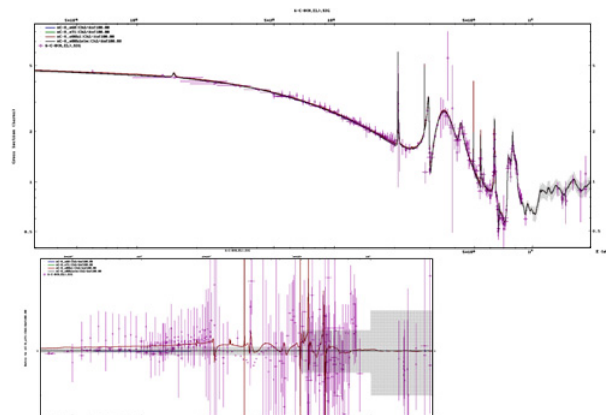


Figure 8. Cross sections for $n+^{\text{nat}}\text{C}$ elastic scattering. The top panel shows ENDF/B-VII.1 (black curve) and the new cross section (red curve) compared to experimental (magenta) points. The bottom panel shows the new cross section and experimental points plotted as a ratio to ENDF/B-VII.1 (figure courtesy of Andrej Trkov).

5. Summary and conclusions

The EDA analyses of reactions in the $^{13,14}\text{C}$ and ^{17}O systems described here give very good fits to all the data included, with values of chi-square per degree of

freedom in the range 1.5–1.7. The neutron cross sections from these analyses are highly constrained by the unitarity property mentioned earlier. For the ^{17}O system, the low-energy $n+^{16}\text{O}$ scattering cross sections are now in better agreement with high-precision measurements, and the (n, α_0) cross section agrees with the data of Bair and Haas [9] and Giorginis [10]. A post-analysis check showed good agreement also with σ_T measurements done at RPI by Danon. The evaluated ^{16}O file CIELO 3/16 = ENDF/B VIII.0- $\beta 2$ extends to 150 MeV, and is the same as ENDF/B VII.1 above 9 MeV (except for capture). The changes in the cross sections from ENDF/B VII.1 appear not to have made much difference in the benchmarks that have been tested so far. Changes in k_{eff} of -50 to -100 pcm have been reported, which is rather surprising, considering the $\approx 40\%$ changes in the reaction cross section. For further discussion of the implications of this new evaluation for the CIELO project, please see the paper of Chadwick, *et al.* [11] in the proceedings of this conference.

The scale of the $^{13}\text{C}(\alpha, n)^{16}\text{O}$ cross section at low energies has been fixed by the ^{17}O analysis, which should lead to a better determination of this important s -process source reaction in astrophysics. We plan further improvements on the astro-physically important $^{16}\text{O}(n, \gamma)$ reaction, by putting in the resonant structure of the capture cross section above the first resonance.

The EDA analysis of the ^{13}C system gave quite reasonable results for the $n+^{12}\text{C}$ cross sections at energies up to about 6.5 MeV, and resolved the large discrepancy between the experimental scales of two recent measurements of the inelastic cross section to the first level (see Fig. 5). The analysis also clarified the level structure of the ^{13}C system in the region around $E_x = 10.9$ MeV.

In recent work on the ^{14}C system, more channels were added to the existing single-channel analysis in extending it to higher energies (20 MeV). Above that energy, we plan to merge with the existing evaluation in the TENDL file. The $^{12,13}\text{C}(n, \gamma)$ cross sections have been improved, and give better agreement with the MACS in the KADoNIS data base (J.-C. Sublet). However, there are questions from

recent benchmarking work on graphite about the value of the thermal cross section for $n+^{13}\text{C}$ capture.

The elastic scattering cross section for natural carbon becomes $\approx 2\%$ larger than ENDF/B VII.1 around 2 MeV. That difference exceeds the maximum estimated uncertainty (0.6%) of the standard cross section at the upper end of its energy range (1.8 MeV), but may be in better agreement with the measurements. These changes in the cross sections for natural carbon produce about a 70 pcm reduction (the right direction) in the reactivity of the HMI006 benchmark set, according to calculations done by Andrej Trkov at the IAEA.

References

- [1] D.C. Dodder, G.M. Hale, and K. Witte, “The Energy Dependent Analysis Code,” Los Alamos National Laboratory, (unpublished, 1972)
- [2] A.M. Lane and R.G. Thomas, *Rev. Mod. Phys.* **30**, 257–353 (1958)
- [3] L. Wolfenstein, *Ann. Rev. Nucl. Sci.* **6**, 43–76 (1956)
- [4] C.S. Schneider, *Acta Cryst.* **A32**, 375–379 (1976)
- [5] M. Ohkubo, Report JAERI-M-86-193 (1987). Data corrected for hydrogen content by A. Plompen (2013)
- [6] C.H. Johnson, J.L. Fowler, N.W. Hill, and J.M. Ortolfo, *Proc. Int. Conf. on Nuclear Cross Sections for Technology, Knoxville* (NBS Spec. Pub. **594**, 1980), 807–811 (1979)
- [7] J.L. Fowler, C.H. Johnson, and R.M. Feezel, *Phys. Rev. C* **8**, 545–562 (1973)
- [8] S. Ciejracks, F. Hinterberger, G. Schmalz, D. Erbe, P. v.Rossen, and B. Leugers, *Nucl. Instr. Meth.* **169**, 185–198 (1980)
- [9] J.K. Bair and F.X. Haas, *Phys. Rev. C* **7**, 1356–1364 (1973)
- [10] G. Giorginis, “IRMM measurement in 2007 of the $^{16}\text{O}(n, \alpha)^{13}\text{C}$ cross section,” personal communication to G. Hale (March, 2016)
- [11] M.B. Chadwick *et al.*, *Proc. ND2016* (this conference, 2016)